Supplementary Information

[(V^{IV}O)_2M^{II}_5] (M = Ni, Co) Anderson wheels

Hector W. L. Fraser,[a] Emily H. Payne,[a] Arup Sarkar,[b] Lucinda R. B. Wilson,[a] Dmitri Mitcov,[c] Gary S. Nichol,[a] Gopalan Rajaraman,*[b] Stergios Piligkos*[c] and Euan K. Brechin*[a]

a. EaStCHEM School of Chemistry, The University of Edinburgh, David Brewster Road, Edinburgh, EH9 3FJ Scotland, UK. E-mail: E.Brechin@ed.ac.uk
b. Department of Chemistry, Indian Institute of Technology Bombay, Powai, Mumbai 400076, India. E-mail: rajaraman@chem.iitb.ac.in
c. Department of Chemistry, University of Copenhagen, Universitetsparken 5, 2100 Copenhagen, Denmark. Email: piligkos@chem.ku.dk
d. WestCHEM School of Chemistry, University of Glasgow, University Avenue, Glasgow G12 8QQ, Scotland, UK.
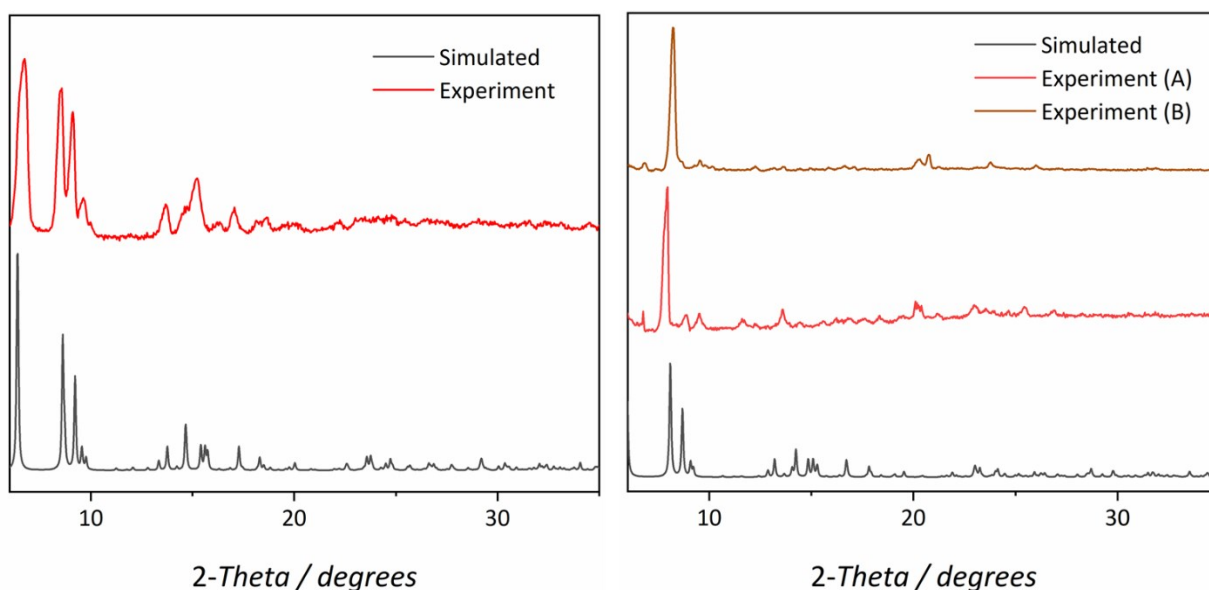
Figure S1. Powder XRD patterns for complex **1** (left) and **2** (right). The latter desolvates rapidly as observed in partially dried sample (A) and fully dried sample (B).

Table S1. Selected structural parameters for the bridging motifs between the metal ion pairs in compound **1**. These include: V-O bond length, M-O bond length, M-Cl bond length, M-O-M bond angle and M-Cl-M bond angle.

	V-O (Å)	M-O (Å)	M-Cl (Å)	M-O-M (°)	M-Cl-M (°)
V1/M1	1.969, 2.057	1.995, 2.094	-	95.93, 102.11	-
V1/M2	2.057, 2.177	2.094, 2.122	-	98.29, 101.24	-
V1/M3	2.014, 2.177	2.028, 2.090	-	96.81, 104.27	-
M1/M3	-	2.041, 2.081	2.405, 2.413	103.18	84.20
M1/M2	-	2.053-2.122	-	95.82, 98.33	-
M2/M3	-	2.041-2.094	-	97.40, 100.28	-

Table S2. Selected structural parameters for the bridging motifs between the metal ion pairs in compound **2**. These include: V-O bond length, M-O bond length, M-Cl bond length, M-O-M bond angle and M-Cl-M bond angle.

|	V-O (Å)	M-O (Å)	M-Cl (Å)	M-O-M (°)	M-Cl-M (°)
V1/M1	1.969, 2.054	2.010, 2.133	-	96.05, 102.98	-
V1/M2	2.054, 2.180	2.115, 2.170	-	99.09, 101.33	-
V1/M3	2.013, 2.180	2.026, 2.126	-	96.68, 105.61	-
M1/M3	-	2.078, 2.108	2.422, 2.455	102.91	84.34
M1/M2	-	2.075-2.170	-	94.18, 97.78	-
M2/M3	-	2.075-2.126	-	97.17, 99.97	-
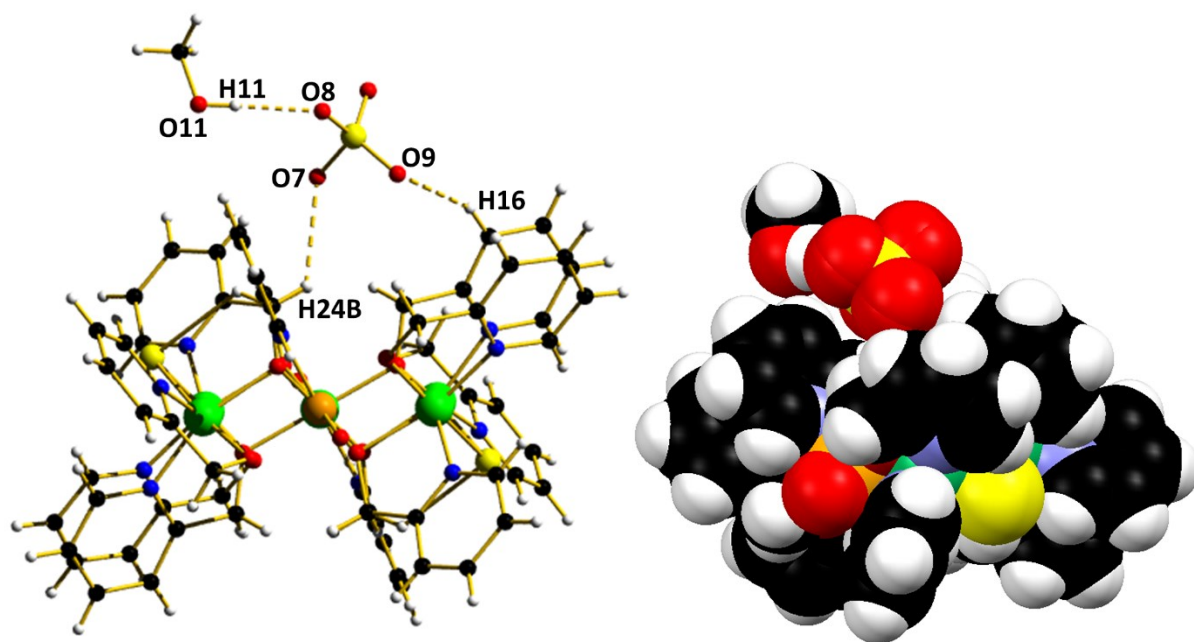
Figure S2. Illustration of the interaction between the MeOH molecules of crystallisation, the ClO_4^- anions and the cation in **1**. Colour code as Figure 1. O8⋯H11 = 2.208 Å, O7⋯H24B = 2.595 Å, O9⋯H16 = 2.595 Å. The image on the right is the equivalent space-fill representation.
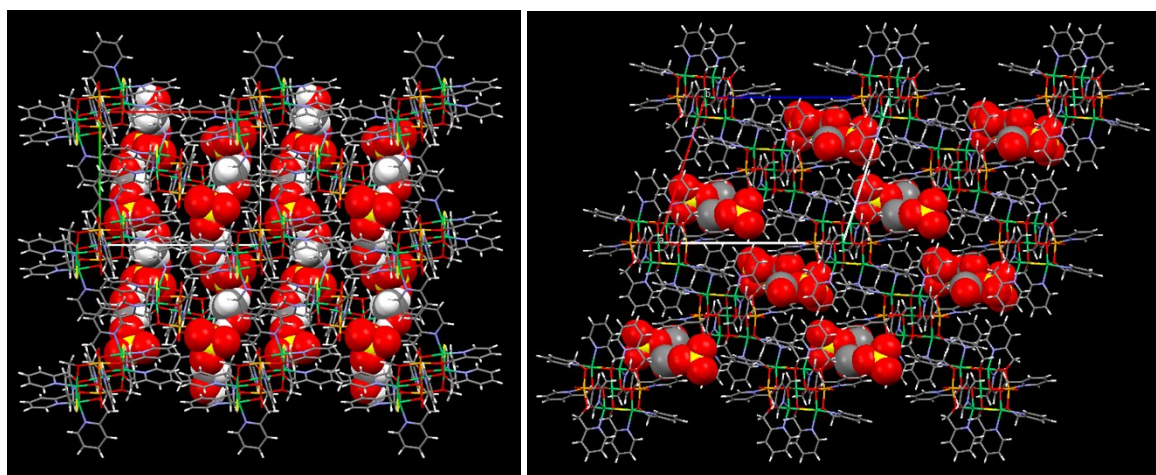

Figure S3. View of the extended structure in complex **1** down the *c* (left) and *b* (right) axes of the unit cell. The anions and solvent of crystallisation are depicted in space-fill and the cluster cations as capped sticks. Colour code as Figure 1.
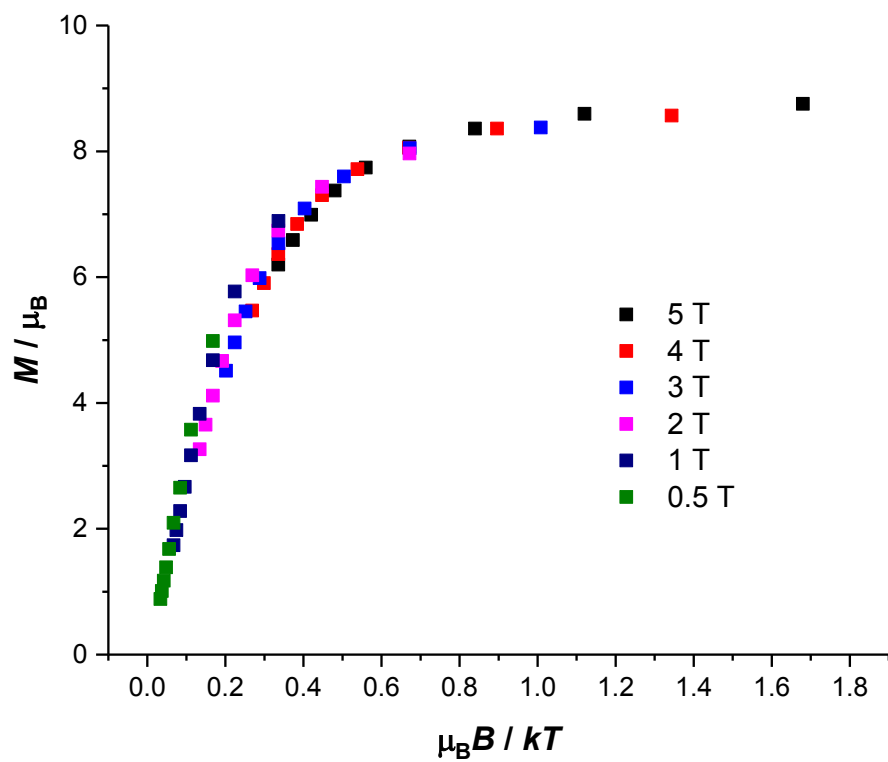
Figure S4. Reduced magnetisation data of **1**, showing no nesting of the VTVB curves, as discussed in the main text.
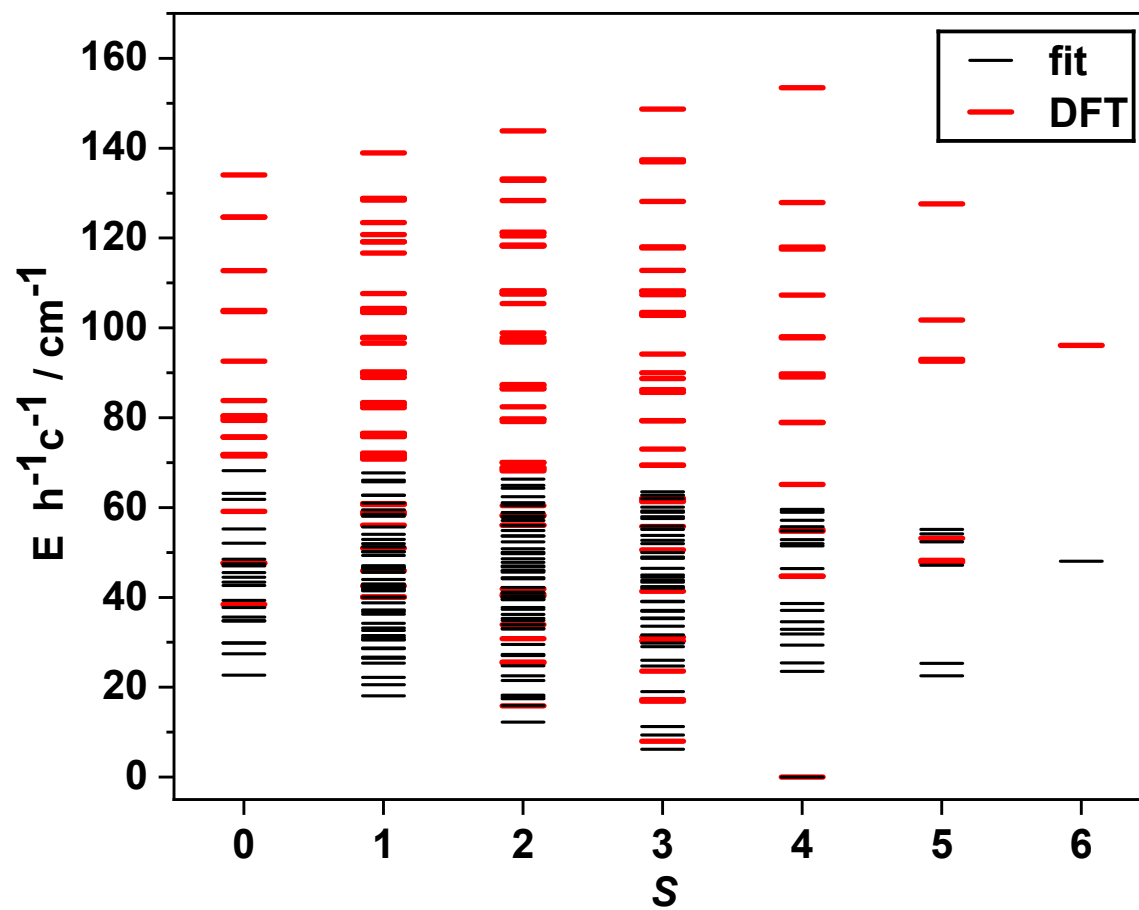
Figure **S5**: Spin eigenstates of **1**, obtained as explained in the main text.
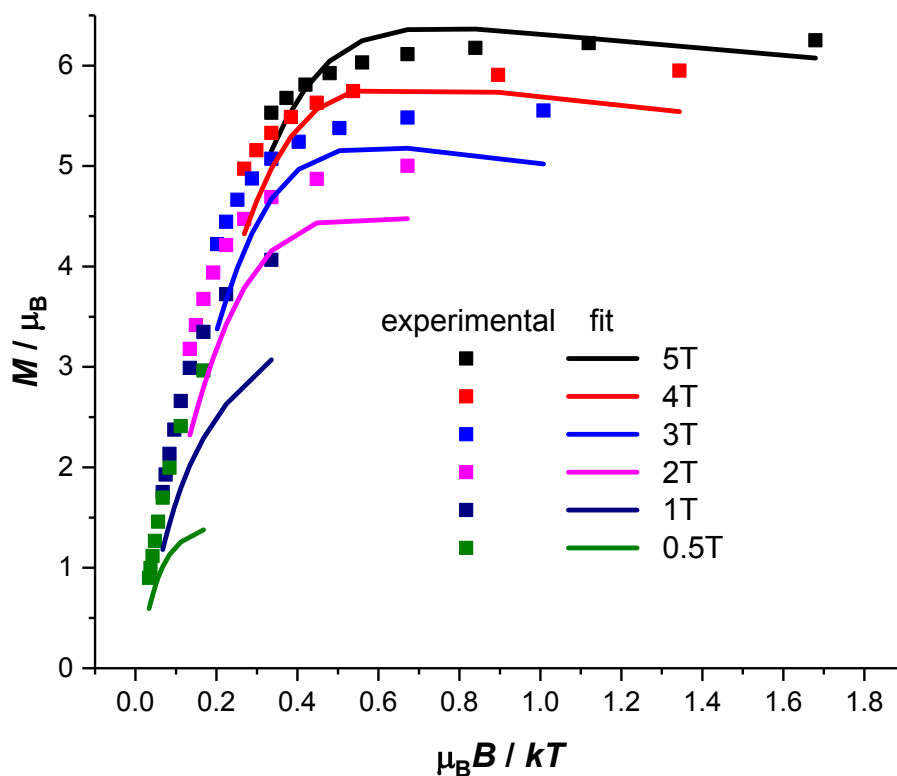
Figure S6. Reduced magnetisation data of **2**, showing significant nesting of the VTVB curves, and failure to model the VTVB curves with the parameters determined from fitting the temperature dependence of the χT product, as discussed in the main text.

Scheme S1. Schematic diagram of the high spin and broken symmetry arrangements of the metal ion spins in **1** and **2** used for DFT calculations.

Table S3. Mulliken spin density values computed from B3LYP/TZV level of theory on the respective Ni^{II} and V^{IV} centres in **1** obtained from high spin and four broken symmetry calculations. The numbers beside the atoms are according to scheme 1.

| Spin density	Ni1(centre)	Ni2	Ni3	Ni4	Ni5	V1	V2	$\langle S^2 \rangle$
HS	1.740	1.677	1.666	1.666	1.677	1.128	1.128	42.05
BS1	1.742	-1.675	1.674	1.674	-1.675	1.127	1.127	10.03
BS2	1.738	1.663	1.671	1.671	1.663	-1.132	-1.132	22.03
BS3	-1.738	1.667	1.677	1.677	1.667	1.129	1.129	22.04
BS4	-1.740	1.671	1.664	1.664	1.671	-1.131	-1.131	10.02
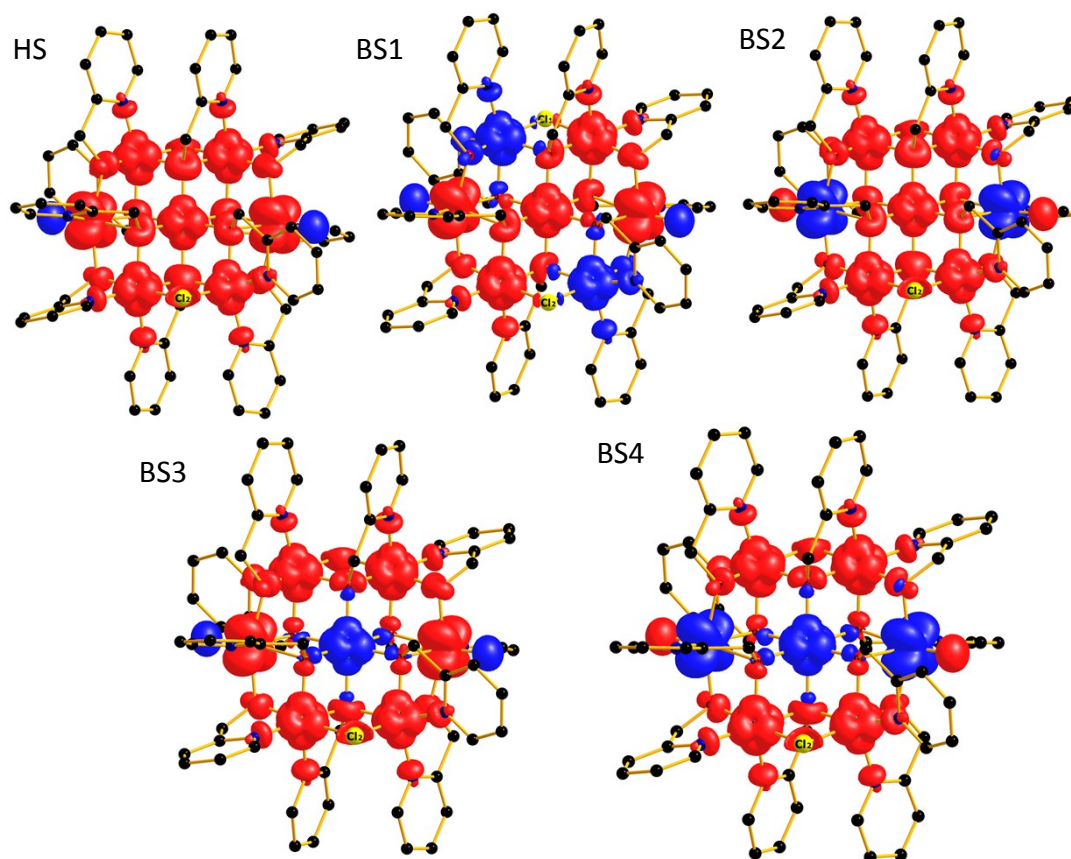
Figure S7. Spin density plots of complex **1** of the HS, BS1, BS2, BS2 (top) and BS3, BS4 (bottom) with an iso-surface value of 0.0065 e/Bohr3. Hydrogen atoms are removed for clarity.

Table S4: Selected overlap integral ($S_{\alpha\beta}$) values between the Ni^{II} and V^{IV} atomic orbitals in **1**.

MO number	Ni (α)	MO number	V (β)	$S_{\alpha\beta}$
403	Ni5($d_{x^2-y^2}$), Ni3(d_{z^2}), Ni2($d_{x^2-y^2}$), Ni4(d_{z^2})	398	V1(d_{xy}), V2(d_{xy})	0.0744
402	Ni5($d_{x^2-y^2}$), Ni3($d_{x^2-y^2}$), Ni2($d_{x^2-y^2}$), Ni4($d_{x^2-y^2}$), Ni1(d_{z^2})	397	V1(d_{xy}), V2(d_{xy})	0.0630
395	Ni5(d_{xz}), Ni3(d_{xz}), Ni2(d_{xz}), Ni4(d_{xz})	397	V1(d_{xy}), V2(d_{xy})	-0.0982
371	Ni5(d_{yz}), Ni3(d_{xy}), Ni2(d_{xy}), Ni4(d_{yz}), Ni1(d_{xz})	397	V1(d_{xy}), V2(d_{xy})	0.0710
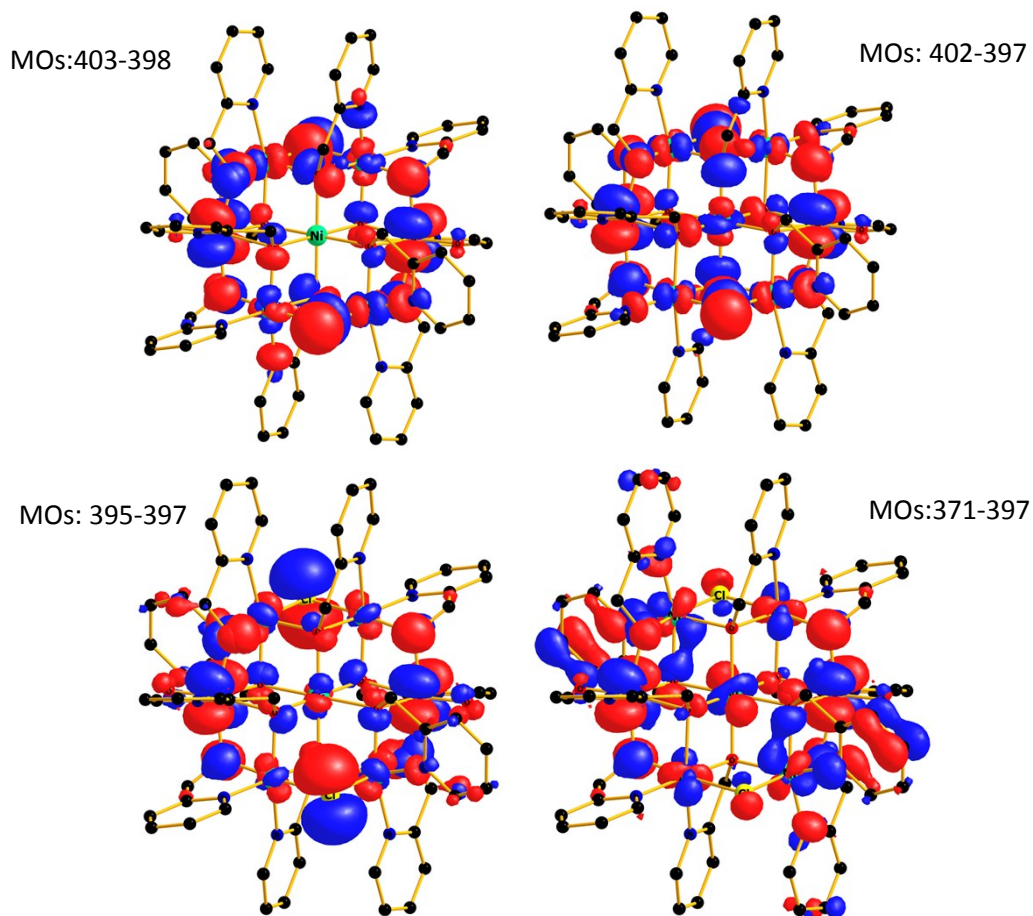
Figure S8. Orbital overlap diagrams of the five Ni(II) centres and two V(IV) centres (iso-surface value 0.03 e/bohr^3) for complex **1**.
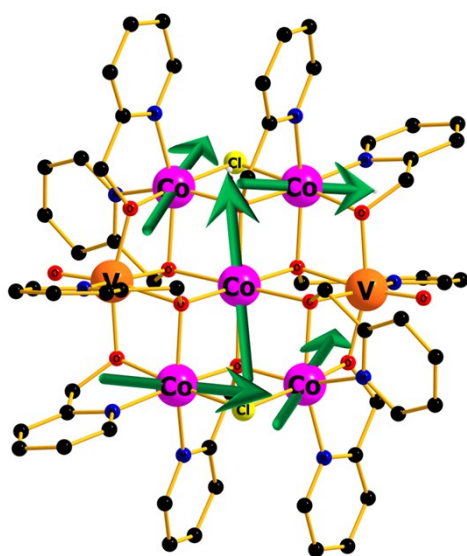
Figure S9. NEVPT2 computed D_{zz} orientations plotted on each Co^{II} ion in complex **2**.

Table S5: Wavefunction analysis, statewise energies and their corresponding contribution towards axial and rhombic ZFS parameters for the central Co^{II} ion (M2 in Figure 1) of complex **2** (only up to 4th excited state shown).

States	Energy (cm^{-1})	CASSCF wavefunction (major contribution)	Contribution to D (cm^{-1})	Contribution to E (cm^{-1})
GS	0.0	$d_{yz}^2 d_{xz}^2 d_{xy}^1 d_{z^2}^1 d_{x^2-y^2}^1$ (58%)	0.00	0.00
1st ES	618.9	$d_{yz}^2 d_{xz}^1 d_{xy}^2 d_{z^2}^1 d_{x^2-y^2}^1$ (46%) $d_{yz}^2 d_{xz}^2 d_{xy}^1 d_{z^2}^1 d_{x^2-y^2}^1$ (15%)	38.0	34.23
2nd ES	1293.5	$d_{yz}^1 d_{xz}^2 d_{xy}^2 d_{z^2}^1 d_{x^2-y^2}^1$ (62%)	24.3	-18.30
3rd ES	6963.4	$d_{yz}^1 d_{xz}^2 d_{xy}^1 d_{z^2}^1 d_{x^2-y^2}^2$ (44%) $d_{yz}^2 d_{xz}^1 d_{xy}^1 d_{z^2}^1 d_{x^2-y^2}^2$ (22%)	6.3	1.21
4th ES	7973.3	$d_{yz}^2 d_{xz}^1 d_{xy}^1 d_{z^2}^1 d_{x^2-y^2}^2$ (44%) $d_{yz}^2 d_{xz}^1 d_{xy}^1 d_{z^2}^2 d_{x^2-y^2}^1$ (22%)	4.0	0.64

Mass Spectrometry

Mass spectrometry was performed on a 12 T SolariXr FT-ICR MS (Bruker Daltonics, Bremen, Germany) with an ESI source. The spectrum was acquired in positive ion mode (ESI+). The broadband spectrum was acquired with 16 summed scans between 98.3 *m/z* and 3000 *m/z.* Samples were solubilized in acetonitrile at 50 µM and sprayed by direct infusion into the ESI source. Data were analysed using MassLynx v4.1 software**.**

Electrospray ionisation mass spectrometry (ESI-MS) was carried out on a solution of **1** dissolved in acetonitrile, with the results showing that compound **1** is stable in solution as $[M]^{2+}$ (Figure S11). The most intense peak in the spectrum corresponds to the ion $[M]^{2+}$ where M = $[(VO)_2Ni_5(hmp)_{10}Cl_2]$ and appears at *m/z* = 788.96. This can be attributed to the unfragmented 2+ cationic part of the complex, after loss of the two perchlorate counter ions and solvated methanol. No other peaks could be identified from the spectrum. The observed solution stability of **1** is in agreement with the findings from the mass spectrometry and solution-state NMR spectroscopy for the related heterometallic Anderson wheels of general formula $[M^{III}_2 M^{II}_5 (hmp)_{12}]^{4+}$ (where M^{III} = Cr, Al and M^{II} = Mn, Fe, Co, Ni, Cu, Zn) as described in reference 11 (main text). Consistent with the PXRD data (Figure S1) the structure of **2** is unstable outside the mother liquor, desolvating rapidly and the mass spectrum of the redissolved powder (in MeCN) shows no sign of the $[M]^{2+}$ (where M = $[(VO)_2Co_5(hmp)_{10}Cl_2]$).
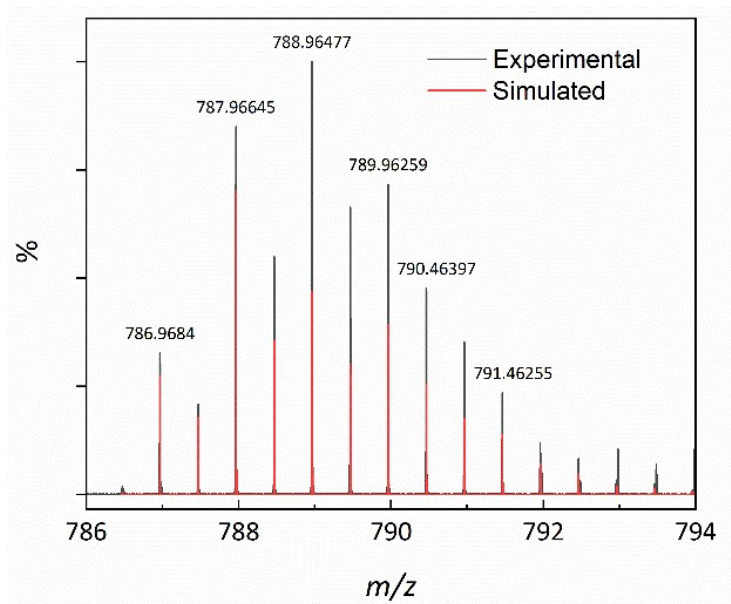
Figure S10. Experimental (black) and simulated (red) peaks for the partial mass spectrum of **1**, showing the unfragmented [M]$^{2+}$ ion.